BMC Veterinary Research

RESEARCH

Open Access

Comparative study of the effects of baicalin and probenecid on microRNA expression profiles in porcine aortic vascular endothelial cells infected by *Glaesserella parasuis*

Ling Guo[1,2,3,4†], Yaqiong Yang[1,4†], Linrong Yang[1,4], Peiyan Sun[1,4], Jing He[2,3], Shulin Fu[2,3], Chun Ye[2,3], Bingbing Zong[2,3] and Yinsheng Qiu[2,3*]

Abstract

Background *Glaesserella parasuis* elicits severe inflammatory responses and vascular damage, thus resulting in high mortality and morbidity in pigs; consequently, early diagnosis and treatment are critical to controlling economic losses. MicroRNAs (miRNAs) have been demonstrated to be involved in vascular endothelial inflammation. Baicalin is an effective Chinese medicinal herb with anti-microbial, anti-inflammatory, and anti-oxidant activity. Probenecid has activity toward multiple mammalian biological processes. Herein, we compared the effects of baicalin and probenecid on the miRNA expression profiles of porcine aortic vascular endothelial cells (PAVECs) infected with *G. parasuis*.

Results We identified 277 known miRNAs and 540 novel miRNAs. Twelve miRNAs were significantly differentially expressed in PAVECs after *G. parasuis* infection. Both baicalin and probenecid affected the miRNA expression profiles in *G. parasuis*-infected PAVECs but showed different modulation patterns. Ssc-miR-27b-5p and ssc-miR-1842 were the top differentially expressed miRNAs (DEmiRNAs) in baicalin group comparing to control group. Ssc-miR-9851-3p and ssc-miR-1296-5p were the top DEmiRNAs in probenecid group. And Ssc-miR-127, ssc-miR-1842, and ssc-miR-9810-3p were the top DEmiRNAs between the baicalin group and probenecid group, as validated by qRT-PCR. The target genes of DEmiRNAs between various groups were subjected to KEGG and GO enrichment analyses. Hematopoietic cell lineage, insulin resistance, and AMPK signaling pathway were the top significantly enriched pathways associated with the target genes of DEmiRNAs in *G. parasuis*-infected PAVECs pretreated with baicalin; in contrast, B cell receptor, T cell receptor, and HIF-1 signaling pathways predominated in *G. parasuis*-infected PAVECs treated with probenecid. We additionally constructed co-expression and protein–protein interaction networks based on the differentially expressed target genes of miR-127, miR-1842, and miR-9810-3p.

Conclusion Our findings suggested that baicalin and probenecid regulated miRNAs associated with vascular inflammation and damage, but showed different modulation patterns. This report provided the first comparison of the effects of baicalin and probenecid on *G. parasuis*-infected PAVECs, and might aid in the development of novel biomarkers and therapeutic targets to control *G. parasuis* infection.

†Ling Guo and Yaqiong Yang contributed equally to this work.

*Correspondence:
Yinsheng Qiu
qiuyinsheng6405@aliyun.com
Full list of author information is available at the end of the article

Keywords *Glaesserella parasuis*, MicroRNA, Inflammation, Baicalin, Probenecid

Background

Glaesserella parasuis (*G. parasuis*), a commensal bacterium in the porcine upper respiratory tract, is the etiological agent of Glässer's disease, causing polyserositis, meningitis, and arthritis, particularly in young piglets under stressful conditions [1, 2]. *G. parasuis* elicits severe inflammatory responses and results in high mortality and morbidity, thus leading to large economic losses in the swine industry [3]. *G. parasuis* infection is initiated through bacterial invasion of host cells, evasion of macrophage phagocytosis, and resistance to complement-mediated bactericidal activity and inflammatory responses [4]. However, the pathogenesis of *G. parasuis* is poorly characterized. Although antibiotics are commonly used in the swine industry to control Glässer's disease, antibiotic resistance is an increasing problem worldwide [5]. Thus, new antibiotic substitutes must urgently be explored to control and prevent *G. parasuis* infection.

Baicalin, a major component isolated from *Scutellaria baicalensis* Georgi (Huangqi), is an effective Chinese medicinal herb with extensive pharmacological effects, including anti-microbial [6, 7], anti-inflammatory [8–10], anti-oxidant [11, 12] and anti-tumor [13] activities. Baicalin has been reported to attenuate lupus autoimmunity by inhibiting mTOR signaling activation, and regulating the differentiation of Tfr cells and Tfh cells [9]. Baicalin also modulates macrophage transformation from pro-inflammatory to anti-inflammatory subsets, and decreases inflammation by inhibiting the JAK/STAT pathway [8]. Recent studies have demonstrated that baicalin attenuates lipopolysaccharide (LPS)-induced inflammation by inhibiting expression of CD14 and activation of the TLR4/NF-κB p65 pathway [14], as well as by regulating the expression of miR-181b and HMGB1 [15]. In a previous study, we have demonstrated that baicalin suppresses reactive oxygen species production, apoptosis, and the NLRP3 and NF-κB signaling pathways during *G. parasuis* infection of porcine aortic vascular endothelial cells (PAVECs), thus inhibiting *G. parasuis*-induced inflammation [16]. We have also demonstrated that baicalin modifies the expression profiles of long non-coding RNAs (lncRNAs), microRNAs (miRNAs), and mRNAs, and consequently regulates inflammatory signaling pathways in *G. parasuis*-infected PAVECs [10, 17].

Probenecid is a competitive inhibitor of organic acid transport in the kidneys and other organs [18]. The primary clinical uses for probenecid are as a uricosuric agent in the treatment of gout. Probenecid has been found to decrease the renal excretion of antibiotics, specifically penicillin [19, 20]. Because of its lack of adverse effects, probenecid is a valuable pharmacological tool in clinical and basic research. Probenecid has been reported to interfere with the function of pannexin-1 cellular membrane channel and increase sperm motility in men with spinal cord injury [21]. Recent studies have suggested that probenecid also has neuroprotective activity, and may be a new treatment option for neurological disorders [22–24]. Furthermore, probenecid has anti-inflammatory and anti-nociceptive functions in the central nervous system [22]. Probenecid has recently been reported to effectively inhibit replication of SARS-CoV-2, influenza virus, and respiratory syncytial virus [25, 26]. Moreover, probenecid has been reported to decrease infection and inflammation in acute *Pseudomonas aeruginosa* pneumonia [27]. In addition, co-administration of probenecid with sulopenem has been used to treat urinary tract infections by multidrug-resistant bacteria [28]. Probenecid has broad activity toward multiple mammalian biological processes. However, whether probenecid might have similar effects to those of baicalin in regulating inflammation responses after *G. parasuis* infection in PAVECs was unknown.

MiRNAs are short endogenous RNAs (19–25 nucleotides) that post-transcriptionally regulate the silencing of target genes [29]. A single miRNA can influence the expression of many genes and participate in multiple functional pathways by targeting hundreds of mRNAs [30]. MiRNAs have been shown to target key pathogenic pathways involved in the inflammatory response and thus are an exciting area of research [31, 32]. They have also been found to regulate the expression of target genes involved in the intestinal barrier in inflammatory bowel disease [33]. In addition, miRNAs suppress fibroblast proliferation and promote fibroblast inflammation during cardiac injury [34]. Furthermore, miRNAs play important roles in modulating mucosal defense, homeostasis, and inflammatory responses in mucosal inflammation [35]; and in inflammatory responses in human placentas under preeclampsia and intrauterine growth restriction [36]. Recent reports have indicated that miRNAs restrict vascular endothelial inflammation in atherosclerosis [37, 38]. Thus, miRNAs might potentially have important roles in regulating inflammation during *G. parasuis* infection of PAVECs and serve as biomarkers for the control of *G. parasuis* infection and vascular inflammation. These possibilities warrant further investigation.

Therefore, in the present study, we used a porcine model of Glässer's disease based on infection of PAVECs with a highly virulent *G. parasuis* strain. To explore the potential functions of baicalin and probenecid on Glässer's disease, we used next generation sequencing to compare the effects of these drugs on the miRNA expression profiles in *G. parasuis*-infected PAVECs. Our findings would enhance understanding

of the molecular mechanisms and effects of baicalin and probenecid on vascular damage and inflammation, and provide a basis for developing new biomarkers and therapeutic targets for *G. parasuis* infection.

Materials and methods

Bacterial strain and drugs

G. parasuis strain SH0165, serovar 5, was a gift from State Key Laboratory of Agricultural Microbiology, Huazhong Agricultural University (Wuhan, China). The strain was isolated and cultured in tryptic soy broth (Difco Laboratories, Franklin Lakes, NJ, USA) or tryptic soy agar (Difco Laboratories) supplemented with nicotinamide adenine dinucleotide at 10 μg/mL (Sigma-Aldrich Corporation, St. Louis, MO, USA) and 10% fetal calf serum (Gibco, Carlsbad, CA, USA) at 37 °C, as previously described [39].

Baicalin was obtained from the National Institutes for Food and Drug Control (Beijing, China; B110715-201318). Before use, the baicalin was diluted to 500 μg/mL in Roswell Park Memorial Institute-1640 medium (Gibco), to serve as a working solution. The final baicalin concentration in the culture medium was 50 μg/mL.

Probenecid was purchased from Selleck.cn (Shanghai, China; S4022) and dissolved in DMSO (Sigma; 4540) to a concentration of 100 mM, to serve as a working solution. The final probenecid concentration in the culture medium was 100 μM.

Porcine aortic vascular endothelial cell isolation and culture

This study was approved by the Animal Care and Use Committee of Wuhan Polytechnical University, Hubei Province, China (WPU202303002). All experimental animals were euthanized intravenously with pelltobarbitalum natricum at the dosing of 80 mg/kg body weight before dissection.

Three 30-day-old naturally farrowed weaning Duroc × Landrace × Large white piglets, weighing 6–8 kg, were obtained from Wuhan COFCO Meat Product Co. Ltd. (Wuhan, China) and used for PAVEC isolation. All piglets tested negative for *G. parasuis* infection, according to an indirect enzyme-linked immunosorbent assay detecting specific antibodies against *G. parasuis* (INGEZIM *Haemophilus* 11. HPS. K1; Inmunología y Genética Aplicada S.A. (INGENASA), Madrid, Spain). The pigs were anaesthetized with nembutal at 80 mg/kg body weight (Qingdao Jiskang Biotechnology, Qingdao, China) through intravenous injection. PAVECs were isolated and cultured as previously described [10, 16].

Drug treatment and *G. parasuis* infection

On the basis of our previous infection model experiment, an MOI of 1:1 was used to construct the model for the inflammatory response triggered by *G. parasuis* infection [16]. PAVECs (1×10^6) were seeded into 24-well plates (Costar, Corning Incorporated, Corning, NY, USA) and pretreated with baicalin at a final concentration of 50 μg/mL 1 h before 1×10^6 CFU *G. parasuis* infection, or treated with probenecid at a final concentration of 100 μM concurrently with *G. parasuis* infection (1×10^6 CFU). Subsequently, all PAVECs were cultured at 37 °C under 5% CO_2 for 12 h. We examined four experimental groups: group 1: PAVECs treated with M-199 medium (negative control); group 2: *G. parasuis*-infected PAVECs without drug treatment (infection control); group 3: *G. parasuis*-infected PAVECs with baicalin pretreatment (baicalin group); group 4: *G. parasuis*-infected PAVECs with probenecid treatment (probenecid group). Each group included three individual replicates. After 12 h of culture, all cells were harvested and washed five times with 1% sterile phosphate-buffered saline before RNA-sequencing.

Small RNA library construction and sequencing

Total RNA from PAVECs was extracted with an mirVana miRNA Isolation Kit (Invitrogen, USA). RNA quality was assessed with an Agilent Bioanalyzer 2100 instrument (Agilent Technologies, USA). After quality control, total RNA was purified with an RNACleanXP Kit (Beckman Coulter, USA) and RNase-Free DNase Set (QIAGEN GmBH, Germany).

The small RNA library was constructed by addition of 3′-end and 5′-end adapters, and reverse transcription was performed with an NEBNext Multiplex Small RNA Library Prep Set for Illumina (NEB, USA). Purified libraries were quantified with a Qubit 2.0 fluorometer (Invitrogen, USA), and the quality was determined with an Agilent Bioanalyzer 2100 instrument (Agilent, USA) Single-end sequencing was performed with the Illumina HiSeqX platform (Illumina, USA).

MicroRNA sequencing data analysis

The raw data were filtered with the FASTX-Toolkit, version: 0.0.13 (http://hannonlab.cshl.edu/fastx_toolkit/index.html). After adapter trimming and removal of low-quality reads and short reads (< 15 nt), clean reads of 18–40 nt were aligned to the reference genome (*Sus scrofa* Scrofa 10.2.dna.toplevel.fa) with Bowtie software (https://bowtie-bio.sourceforge.net/index.shtml). MiRNAs and other small RNAs were identified according to the information for known miRNAs in the miRBase database (https://www.mirbase.org). After alignment,

non-miRNA reads (rRNA, tRNA, snoRNA, and snRNA) were discarded. The miRCat tool in the sRNA Toolkit package (http://srna-workbench.cmp.uea.ac.uk/tools/analysis-tools/mircat) was used to predict novel miRNAs.

Principal component analysis was used to analyze the relevance of the measured expression levels [40]. Differentially expressed miRNAs (DEmiRNAs) were identified with edgeR [41], on the basis of a fold-change ≥ 2 and p-value ≤ 0.05, which was considered significant. Multiple hypothesis tests were performed to compare the differential expression among the four groups; the p-value threshold was determined according to the false discovery rate (FDR). The miRNA reads were normalized by the trimmed mean of M values (TMM) and then converted to transcripts per million (TPM). The fold change was calculated according to the TPM value.

MicroRNA target prediction and functional analysis

The potential target genes of the DEmiRNAs were predicted with miRanda (http://www.microrna.org/microrna/getDownloads.do). These target genes were then subjected to GO [42] and KEGG [43] enrichment analyses. The target genes were mapped to each term within the GO database. GO terms with corrected p-values ≤ 0.05 and KEGG pathways with q-values ≤ 0.05 were considered significantly enriched.

The co-expression network of the DEmiRNAs and their potential targets was constructed on the basis of detection of similar expression patterns. Pearson's correlation coefficient and the corresponding p-value were determined with the WGCNA R software package (https://horvath.genetics.ucla.edu/html/CoexpressionNetwork/Rpackages/WGCNA/index.html). For visual representation, only the strongest correlations (correlation coefficient > 0.9 or < −0.9 and p < 0.05) were retained to construct the co-expression network with Cytoscape software (https://cytoscape.org).

The target genes of the DEmiRNAs were analyzed with the STRING database (https://cn.string-db.org). A protein–protein interaction (PPI) network was built and visualized with Cytoscape software.

Quantitative RT-PCR

Total RNA containing small RNA was isolated from PAVECs by using mirVana miRNA Isolation Kit (Invitrogen). Reverse transcription was performed with the Mir-X miRNA First-Strand Synthesis Kit (Takara, China). Quantitative real-time PCR (qRT-PCR) was performed as previously described, with U6 as the reference gene for miRNAs. To validate the reliability of the sequencing data, we also tested the relative expression levels of two differential coding genes (HBEGF and TOP2A). Primers used in this study are shown in Table 1, and the universal reverse primer was provided by the Mir-X kit.

Table 1 Primers used for qRT-PCR validation

Gene	Nucleotide Sequence (5′–3′)		Tm (°C)
ssc-miRNA-127	Forward	CGTCGGATCCGTCTGAGC	59.1
	Reverse	AGTGCAGGGTCCGAGGTATT	
ssc-miRNA-1842	Forward	GCGTTGGCTCTGCGAGG	58.9
	Reverse	AGTGCAGGGTCCGAGGTATT	
ssc-miRNA-9810-3p	Forward	GCGAGCACGCGGCCA	59.6
	Reverse	AGTGCAGGGTCCGAGGTATT	
ssc-miR-1296-5p	Forward	TTAGGGCCCTGGCTCCATCTCC	64
	Reverse	AGTGCAGGGTCCGAGGTATT	
ssc-miR-27b-5p	Forward	AGAGCTTAGCTGATTGGT GAACA	59
	Reverse	AGTGCAGGGTCCGAGGTATT	
U6	Forward	CTCGCTTCGGCAGCACA	60
	Reverse	AACGCTTCACGAATTTGCGT	
HBEGF	Forward	GGCAGACCTGGACCTTTTGA	59.7
	Reverse	CACGTACTTGCACTCTCCGT	
TOP2A	Forward	TCAAACGAAATGACAAGCGAG	60
	Reverse	AACTGACCAATGGGCTGTAAGA	
β-actin	Forward	TGCGGGACATCAAGGAGAAG	60
	Reverse	AGTTGAAGGTGGTCTCGTGG	

Statistical analysis

The data are shown as mean ± SD. Differences were analyzed with two-tailed Student's t-test. Differential expression with p < 0.05 was considered significant.

Results

General statistics of miRNA sequencing data

Deep sequencing was performed to explore miRNA expression profiles in PAVECs with the Illumina HiSeqX platform. A total of 19,990,406 ± 1,747,639 raw reads from the negative control group (group 1), 23,080,911 ± 2,168,993 raw reads from the infection control group (group 2), 21,461,310 ± 643,000 raw reads from the baicalin-treated group (group 3), and 19,736,515 ± 808,521 raw reads from the probenecid-treated group (group 4) were obtained (Table 2). After elimination of adapters and low-quality reads, clean reads were obtained, with a clean ratio ranging from 90.74% to 95.86% (Table 2). Furthermore, in the miRbase database, we identified 14,256,004 ± 1,322,092 clean reads from the negative control group, 13,712,141 ± 1,551,808 clean reads from the infection control group, 12,933,168 ± 730,320 clean reads from the baicalin-treated group; and 11,379,398 ± 298,186 clean reads from the probenecid-treated group (Table 2). The read length and count distribution in the four groups widely varied,

Table 2 Statistical summary of high-throughput sequencing data in PAVECs

Sample ID	Raw reads	Clean reads	Clean ratio (%)	all reads	miRbase	rRNA	tRNA	snoRNA	snRNA	mRNA
Control-1	21,317,664	20,420,831	95.79%	17,135,824	15,067,759	353,410	8,777	84,226	10,227	245,294
Control-2	20,643,224	19,788,145	95.86%	16,994,591	14,969,822	367,404	16,957	74,960	9,607	239,383
Control-3	18,010,330	17,181,466	95.40%	14,569,083	12,730,432	353,265	18,977	67,925	8,034	218,701
GPS-1	25,200,618	23,890,022	94.80%	18,262,232	15,474,712	417,622	26,013	81,589	9,466	328,972
GPS-2	20,865,781	19,290,080	92.45%	15,007,824	12,551,362	414,145	39,460	78,651	9,012	317,496
GPS-3	23,176,334	21,062,104	90.88%	15,816,178	13,110,349	435,118	46,734	94,019	13,269	364,962
GPS-BA50-1	22,080,979	20,347,773	92.15%	16,288,025	13,167,179	369,733	20,997	104,084	11,596	362,788
GPS-BA50-2	20,797,277	19,120,467	91.94%	15,046,554	12,114,524	379,192	22,579	91,706	10,535	340,802
GPS-BA50-3	21,505,674	19,514,984	90.74%	15,996,383	13,517,800	231,179	9,527	74,920	9,690	312,795
GPS-Probenecid-1	20,131,413	18,983,658	94.30%	14,356,661	11,500,601	536,846	28,734	85,647	11,973	317,777
GPS-Probenecid-2	18,806,435	17,738,433	94.32%	13,551,893	11,039,696	413,543	22,660	79,748	9,988	287,821
GPS-Probenecid-3	20,271,696	18,505,175	91.29%	14,235,786	11,597,897	418,881	26,487	76,109	10,458	324,372

Group 1 (Control-1, 2, 3): PAVECs only;

Group 2 (GPS-1, 2, 3): *G. parasuis*-infected PAVECs (1×10^6 CFU/mL);

Group 3 (GPS-BA50-1, 2, 3): *G. parasuis*-infected PAVECs with baicalin (50 μg/mL) pretreatment

Group 4 (GPS-Probenecid-1, 2, 3): *G. parasuis*-infected PAVECs with probenecid (100 μM) treatment

ranging from 18 to 40 nt. From our result, small RNAs were abundant among the 21–23 nt reads, and were predominantly 22 nt, the typical size of dicer-derived products (Supplemental Figure S1).

Identification of known and novel miRNAs

Alignment to sequences of known miRNAs in the miRBase database led to identification of 277 known miRNAs (Supplemental Table S1). The top ten most abundant miRNAs in the 12 libraries were ssc-miR-126-3p, ssc-miR-126-5p, ssc-miR-125b, ssc-let-7f-5p, ssc-miR-16, ssc-let-7a, ssc-miR-21-5p, ssc-let-7c, ssc-miR-27b-3p, and ssc-miR-125a. In addition, 540 novel miRNAs with $p < 0.05$ were identified in our small RNA deep-sequencing libraries with the miRCat tool, 259 of which had $p < 0.01$ (Supplemental Table S2). Of these 259 novel miRNAs, the top five most abundant miRNAs were novel.29, novel.234, novel.393, novel.449, and novel.534 (Supplemental Table S2). Figure 1 shows the putative secondary structures of these five novel miRNAs. Differential expression analysis indicated that only novel.234 and novel.499 showed differential expression in the multiple comparison. Novel.234 was differentially expressed in group 3 vs. group 4, and had 1429 putative target genes, whereas novel.449 was differentially expressed in group 3 vs. group 1, and had 5148 putative target genes (Supplemental Table S10).

Effects of baicalin on miRNA expression in *G. parasuis*-infected PAVECs

To evaluate the effects of baicalin on the miRNA expression profile in *G. parasuis*-infected PAVECs, we first analyzed the differential miRNA expression between *G. parasuis*-infected PAVECs and un-infected PAVECs (group 2 vs. group 1). After normalization of the data, we identified 12 miRNAs that were significantly differentially expressed in *G. parasuis*-infected PAVECs compared with un-infected PAVECs: eight upregulated and four downregulated (fold change > 2, $p < 0.05$) (Fig. 2A, Supplemental Table S3). In *G. parasuis*-infected PAVECs, the top two upregulated miRNAs were ssc-miR-146a-5p and ssc-miR-146a-3p, whereas the top two downregulated miRNAs were novel.257 and novel.258 (Supplemental Table S3). In PAVECs pretreated with baicalin, compared with those without baicalin pretreatment (group 3 vs. group 2), six miRNAs were significantly differentially expressed: three upregulated and three downregulated (fold change > 2, $p < 0.05$) (Fig. 2B, Supplemental Table S4). Among these six DEmiRNAs, ssc-miR-27b-5p was the top upregulated miRNA, whereas ssc-miR-1842 was the top downregulated miRNA (Supplemental Table S4).

Effects of probenecid on miRNA expression in *G. parasuis*-infected PAVECs

To investigate the effects of probenecid on miRNA expression, we compared the miRNA expression profiles of *G. parasuis*-infected PAVECs with vs. without probenecid treatment (group 4 vs. group 2). Eight miRNAs were significantly differentially expressed between the probenecid-treated group (group 4) and infection group (group 2): seven upregulated and one downregulated (fold change > 2, $p < 0.05$) (Fig. 2C, Supplemental Table S5). Among these DEmiRNAs, ssc-miR-9851-3p

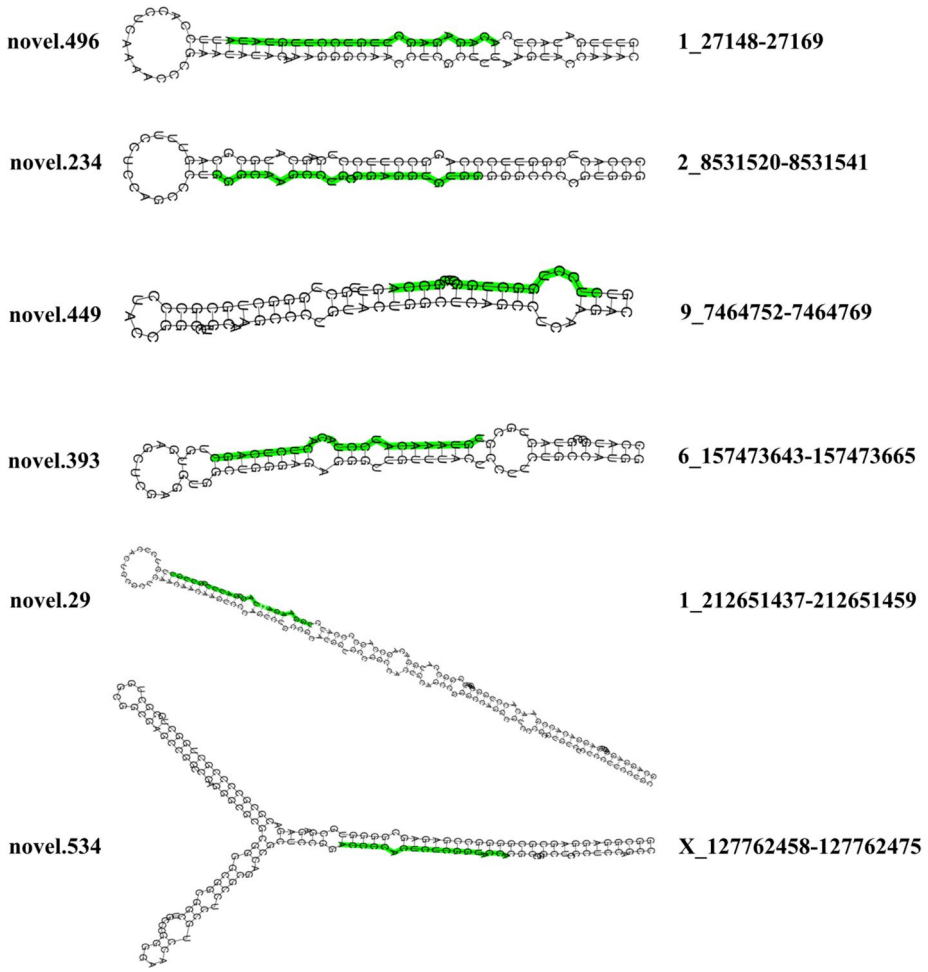

Fig. 1 Predicted secondary structures of the five most abundant novel miRNAs in pigs. The mature sequence is indicated in green

and ssc-miR-1296-5p were the top upregulated miRNAs, whereas novel.437 was the only downregulated miRNA (Supplemental Table S5).

Comparison of effects between baicalin and probenecid

After confirming that both baicalin and probenecid modulated the miRNA expression profiles in *G. parasuis*-infected PAVECs, we further compared the effects of baicalin and probenecid treatment on the miRNA expression profiles in *G. parasuis*-infected PAVECs (group 3 vs. group 4). Six miRNAs were significantly differentially expressed in the baicalin-treated group (group 3) compared with the probenecid-treated group (group 4): five downregulated and one upregulated (fold change > 2, $p < 0.05$) (Fig. 2D, Supplemental Table S6). Among these DEmiRNAs, ssc-miR-127 and ssc-miR-1842 were the top two downregulated miRNAs, whereas ssc-miR-9810-3p was the only upregulated miRNAs (Supplemental Table S6).

Target prediction and functional enrichment analysis

To better understand the functions of the DEmiRNAs, we predicted the interactions between these DEmiRNAs and their putative target genes with miRanda software [44]. A total of 7,904 putative target genes were predicted for the 12 DEmiRNAs in *G. parasuis*-infected PAVECs (Supplemental Table S7). A total of 5,574 putative targets were predicted for the six DEmiRNAs in the baicalin-treated group, whereas 11,418 putative targets were predicted for the eight DEmiRNAs in the probenecid-treated group (Supplemental Table S8, S9). A total of 10,105 putative targets were predicted for the six DEmiRNAs between the baicalin-treated group and probenecid-treated group (Supplemental Table S10).

Different target-gene sets, the putative targets of DEmiRNAs from different comparisons, were used to perform GO and KEGG enrichment analyses. In the GO enrichment results from all four comparisons, cellular process, metabolic process, and single-organism process were the top three terms in the biological process

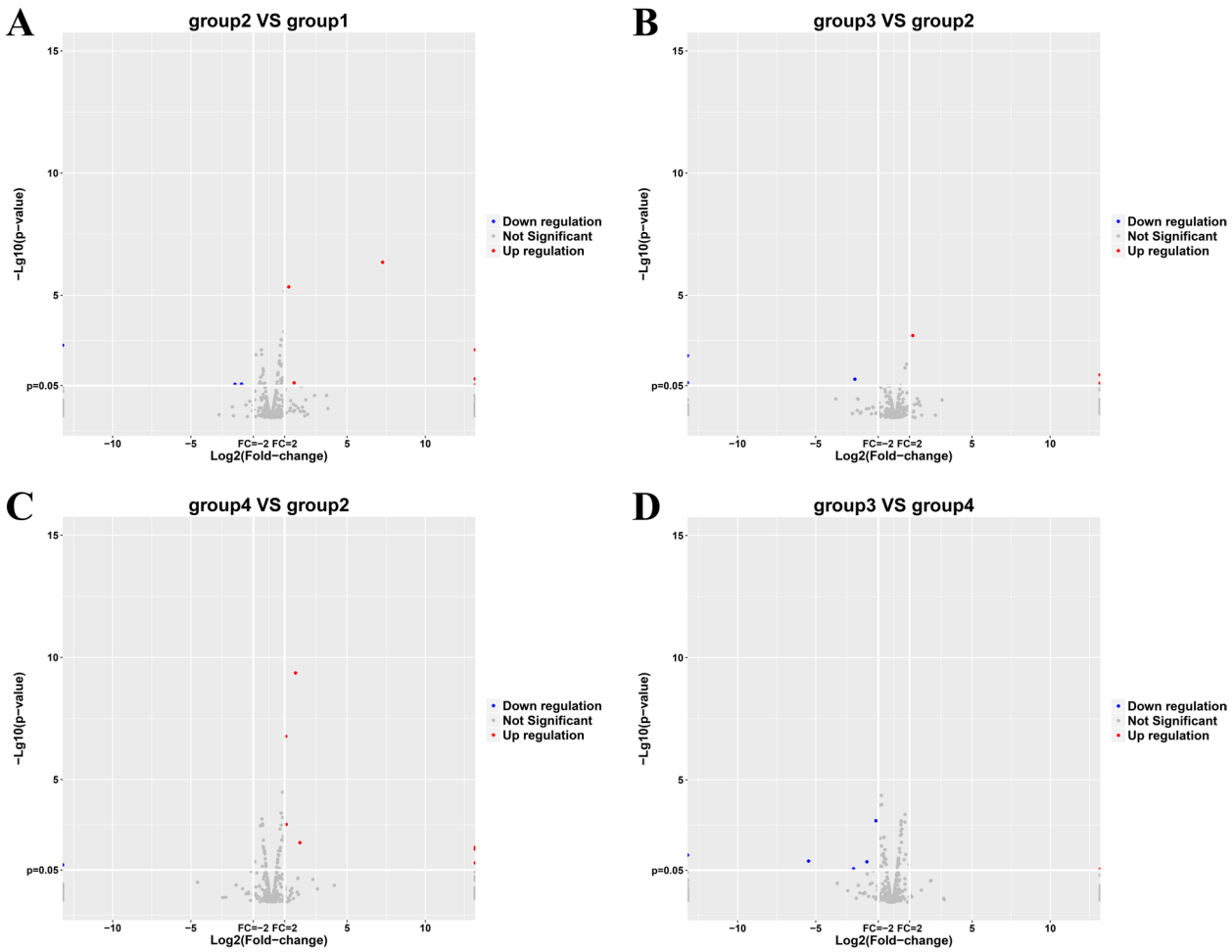

Fig. 2 Volcano plots of the differentially expressed miRNAs (DEmiRNAs) in PAVECs. **A** DEmiRNAs in *G. parasuis*-infected PAVECs vs. control PAVECs. **B** DEmiRNAs in baicalin-treated PAVECs (group 3) vs. *G. parasuis*-infected PAVECs (group 2). **C** DEmiRNAs in probenecid-treated PAVECs (group 4) vs. *G. parasuis*-infected PAVECs (group 2). **D** DEmiRNAs in baicalin-treated PAVECs (group 3) vs. probenecid-treated PAVECs (group 4)

category; cell, cell part, and organelle were the most abundant terms in the cellular component category; and binding and catalytic activity were the top terms in the molecular function category (Fig. 3A, C and Fig. 4A, C). However, the KEGG enrichment results varied among the group comparisons. In group 2 vs. group 1, the target genes of DEmiRNAs in *G. parasuis*-infected PAVECs were enriched primarily in the pathways of hematopoietic cell lineage and proteoglycans in cancer signaling pathways (Fig. 3B). In group 3 vs. group 2, hematopoietic cell lineage, insulin resistance, and the AMPK signaling pathway were the most significantly enriched pathways associated with the target genes of DEmiRNAs in *G. parasuis*-infected PAVECs pretreated with baicalin (Fig. 3D). Notably, in group 4 (treated with probenecid) vs. group 2 (infection control), the target genes of DEmiRNAs were associated primarily with the B cell receptor signaling pathway, T cell receptor signaling pathway, HIF-1 signaling pathway, and proteoglycans in cancer (Fig. 4B). In a comparison of the effects of baicalin and probenecid (group 3 vs. group 4), hematopoietic cell lineage and insulin resistance were the most significantly enriched pathways (Fig. 4D).

Co-expression analysis of DEmiRNAs and their targets

To further explore the differential effects of baicalin and probenecid on *G. parasuis*-infected PAVECs, we selected the most affected DEmiRNAs (ssc-miR-127, ssc-miR-1842, and ssc-miR-9810-3p) from the comparison of the baicalin group vs. probenecid group, and performed co-expression analysis on these miRNAs and their putative target genes. We first used the target genes showing differential expression in any two-group comparison as an input. The results indicated that ssc-miR-127 was associated with 84 differentially expressed targets, ssc-miR-1842 was associated with 158 differentially

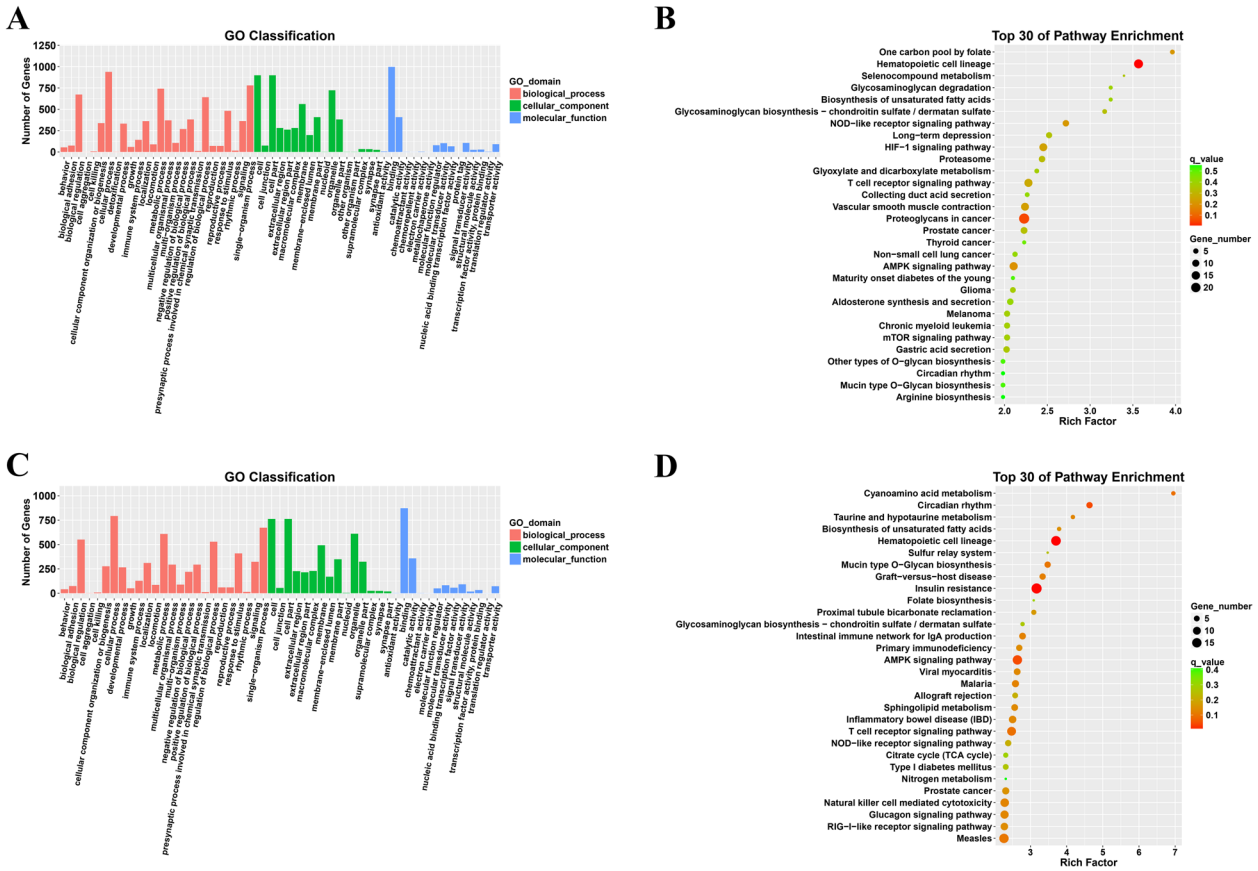

Fig. 3 GO and KEGG enrichment analyses of the target genes of DEmiRNAs miRNAs (l). **A** GO functional enrichment analysis of the target genes of DEmiRNAs in *G. parasuis*-infected PAVECs (group 2) vs. control PAVECs (group 1). **B** KEGG enrichment analysis of the target genes of DEmiRNAs in *G. parasuis*-infected PAVECs (group 2) vs. control PAVECs (group 1). **C** GO functional enrichment analysis of the target genes of DEmiRNAs in baicalin-treated PAVECs (group 3) vs. *G. parasuis*-infected PAVECs (group 2). **D** KEGG enrichment analysis of the target genes of DEmiRNAs in baicalin-treated PAVECs (group 3) vs. *G. parasuis*-infected PAVECs (group 2)

expressed targets, and ssc-miR-9810-3p was associated with 17 differentially expressed targets (Fig. 5A). Subsequently, we selected the target genes showing differential expression in only the comparison of the baicalin group vs. the probenecid group. The results indicated that ssc-miR-127 and ssc-miR-1842 were associated with 24 differentially expressed targets, and ssc-miR-9810-3p was associated with four differentially expressed targets (Fig. 5B, Supplemental Table S11).

Protein–protein interaction network for the differentially expressed targets of DEmiRNAs

We next used the STRING database to analyze the functional associations among the targets of the most affected DEmiRNAs (ssc-miR-127, ssc-miR-1842, and ssc-miR-9810-3p) between the baicalin group and the probenecid group. Twelve differentially expressed target genes were identified in the PPI network (Fig. 6). The target genes encoding EXO1, DLGAP5, CEP55, SPC25, TOP2A, BARD1, E2F7, and UNG were interrelated, whereas HBEGF and CSF2 and SMPD3 and CHST3 were associated with each other separately (Fig. 6A). The node degree was used to evaluate the crucial roles of proteins in the network, and the top connected proteins were found to be EXO1 and DLGAP5 (Fig. 6B).

Validation of differential expression by qRT-PCR

The differential expressions of the top significant DEmiRNAs (ssc-miRNA-127, ssc-miRNA-1842, ssc-miR-9810-3p, ssc-miR-1296-5p, and ssc-miR-27b-5p) and two significant coding genes (HBEGF and TOP2A) were validated in PAVECs by qRT-PCR. As shown in Fig. 7, the expression levels of ssc-miRNA-127, ssc-miRNA-1842, and ssc-miR-9810-3p, with respect to those in the *G. parasuis* infection group, were significantly upregulated after *G. parasuis infection* and significantly downregulated under probenecid treatment (Fig. 7). After treatment with baicalin, ssc-miRNA-127 and ssc-miRNA-9810-3p were significantly downregulated, but ssc-miRNA-1842 showed no significant change between the baicalin group

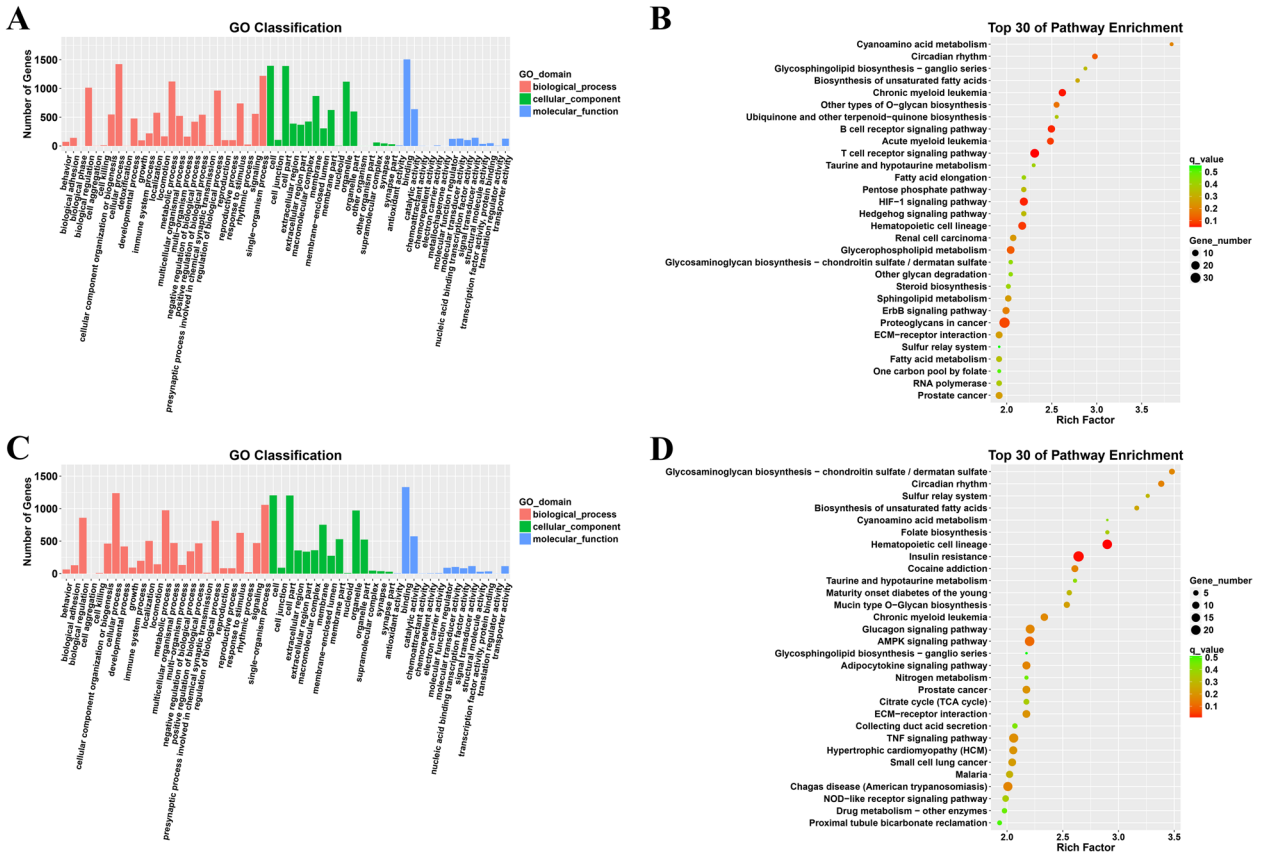

Fig. 4 GO and KEGG enrichment analyses of the target genes of DEmiRNAs (II). **A** GO functional enrichment analysis of the target genes of DEmiRNAs in probenecid-treated PAVECs (group 4) vs. *G. parasuis*-infected PAVECs (group 2). **B** KEGG enrichment analysis of the target genes of DEmiRNAs in probenecid-treated PAVECs (group 4) vs. *G. parasuis*-infected PAVECs (group 2). **C** GO functional enrichment analysis of the target genes of DEmiRNAs in baicalin-treated PAVECs (group 3) vs. probenecid-treated PAVECs (group 4). **D** KEGG enrichment analysis of the target genes of DEmiRNAs in baicalin-treated PAVECs (group 3) vs. probenecid-treated PAVECs (group 4)

and *G. parasuis* infection group (Fig. 7). The expression levels of ssc-miRNA-1296-5p and ssc-miRNA-27b-5p showed the opposite trends of change with ssc-miRNA-127, ssc-miRNA-1842, and ssc-miR-9810-3p (Fig. 7). And the expression levels of HBEGF and TOP2A were consistent with the sequencing data (Fig. 7). However, all these findings will require further validation in future functional studies.

Discussion

G. parasuis infection is prevalent in swine populations, yet many cases remain undiagnosed, potentially leading to severe endothelial damage and systemic complications [1, 2]. This study compared the effects of baicalin and probenecid on the miRNA expression profiles in *G. parasuis*-infected PAVECs, providing a basis for the development of new biomarkers and offering novel insights into the prevention and treatment of *G. parasuis* infection.

MicroRNAs have been reported to participate in the regulation of inflammatory responses in cancer [45] and to play important roles in restricting vascular endothelial inflammation in atherosclerosis [37, 38]. However, the roles of miRNAs in vascular damage and endothelial inflammation during *G. parasuis* infection in piglets were unclear. Moreover, a suitable antibiotic substitute is urgently needed to alleviate the inflammation induced by *G. parasuis* infection in Glässer's disease. Therefore, we used a porcine aortic vascular endothelial cell model to verify the mechanism of inflammatory damage caused by *G. parasuis* infection, and compared the effects of baicalin and probenecid on the expression profiles of miRNAs in *G. parasuis*-infected PAVECs. We explored the potential functions of these two treatments on Glässer's disease through next generation sequencing and bioinformatic analysis. This study represents the first investigation into the comparative analysis of miRNA expression profiles in *G. parasuis*-infected PAVECs following treatment with either baicalin or probenecid, elucidating the differential effects induced by these two drugs.

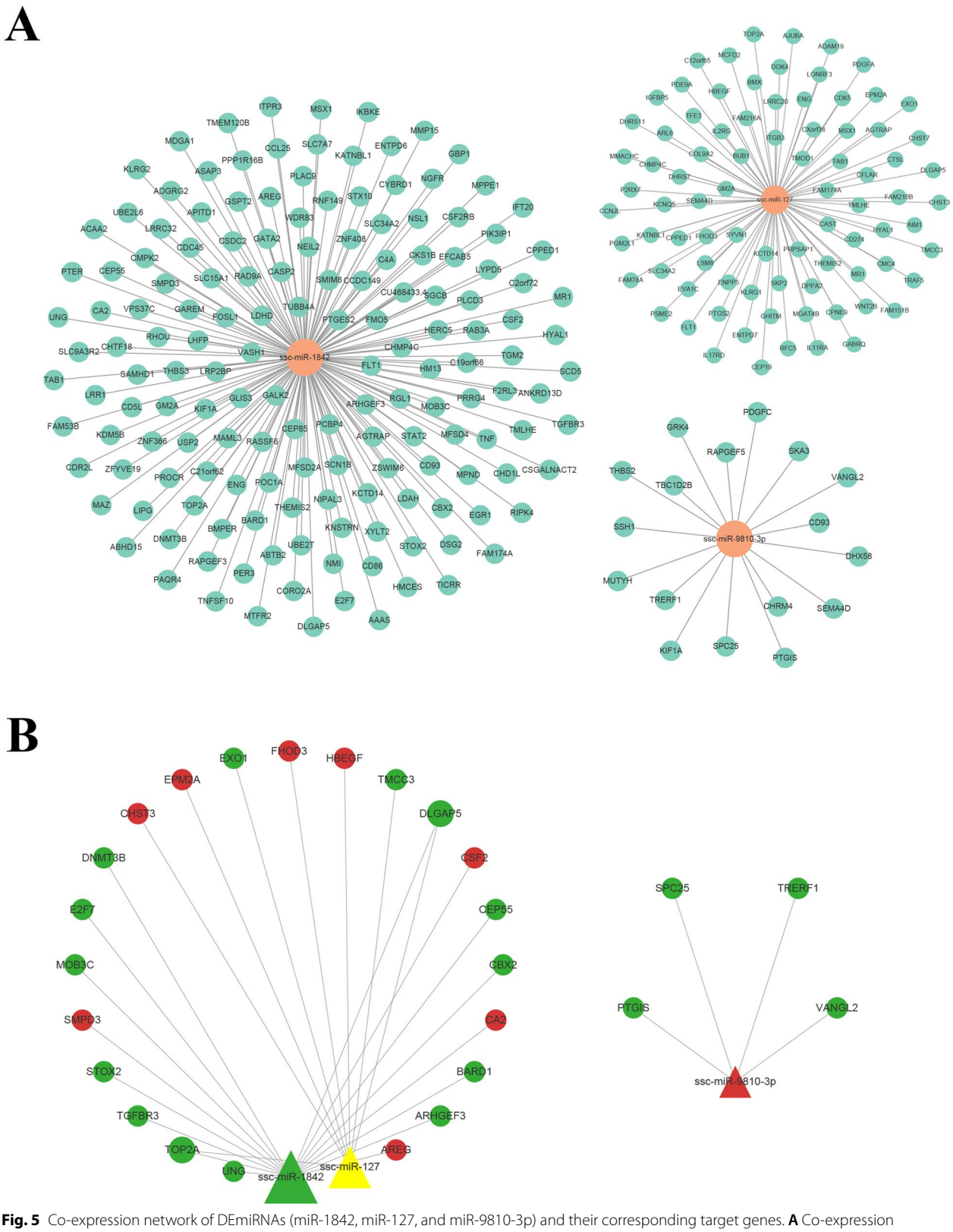

Fig. 5 Co-expression network of DEmiRNAs (miR-1842, miR-127, and miR-9810-3p) and their corresponding target genes. **A** Co-expression of DEmiRNAs with their target genes showing differential expression in comparisons between any two groups. **B** Co-expression of DEmiRNAs with their target genes showing differential expression in only the baicalin group vs. probenecid group

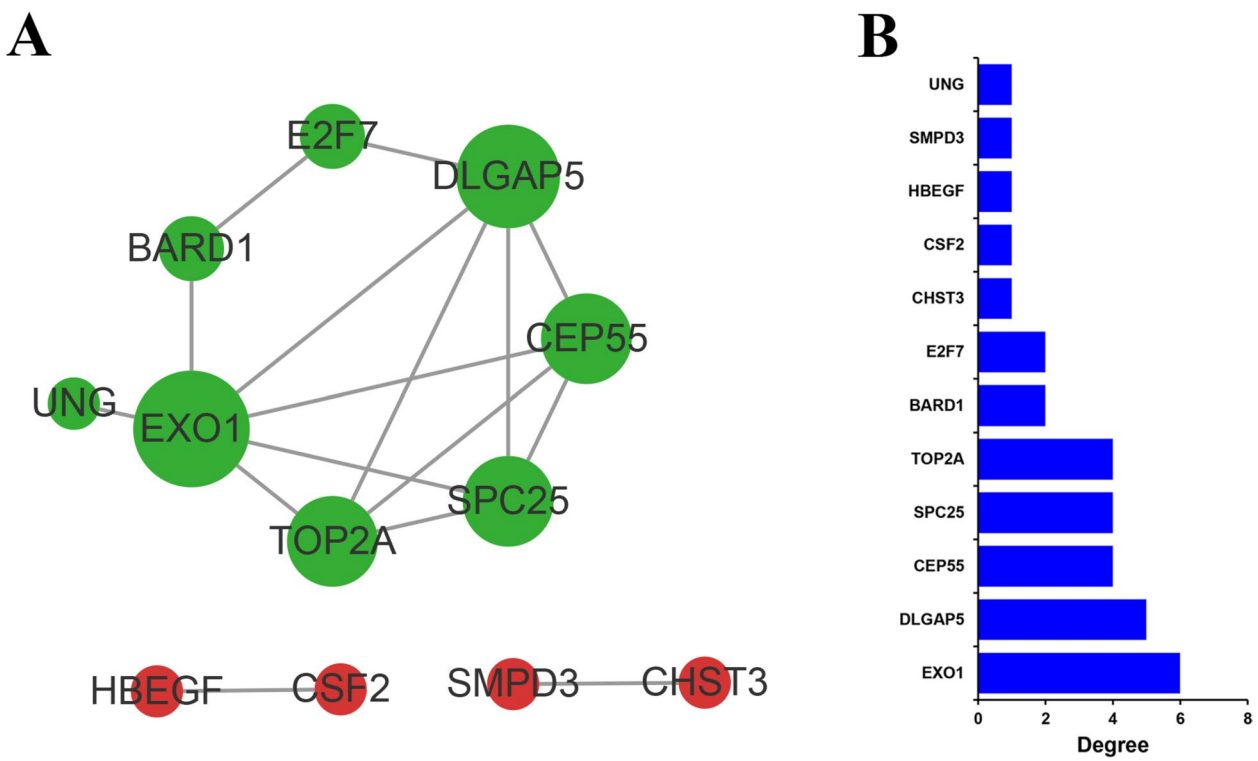

Fig. 6 PPI for differentially expressed targets of DEmiRNAs (miR-1842, miR-127, and miR-9810-3p), based on STRING analysis. **A** PPI network constructed with 12 differentially expressed targets of miR-1842, miR-127, and miR-9810-3p. Nodes represent genes, and edges represent interactions. Node size represents the node degree. **B** Node degrees corresponding to each node in the network, which represent the interaction times for each node. The vertical axis shows the gene name, and the horizontal axis shows the node degree

The top two upregulated miRNAs in *G. parasuis*-infected PAVECs were ssc-miR-146a-5p and ssc-miR-146a-3p, in agreement with our previous results [17]. miR-146a-5p has been reported to function as an anti-inflammatory factor in porcine intestinal epithelial cells and to promote epithelial regeneration during LPS stimulation [46]. Furthermore, miR-146a-5p has been demonstrated to increase the level of autophagy, inhibit pyroptosis of microglia, and attenuate inflammatory pain through human umbilical cord mesenchymal stem cells [47]. Downregulation of miR-146a-3p has been found to attenuate lipopolysaccharide-induced acute lung injury, and to alleviate the inflammatory response and oxidative stress in the lungs in rats by mediating the NF-κB pathway [48]. On the basis of previous reports combined with our results, we speculated that miR-146a-5p and miR-146a-3p might play important roles in vascular damage and inflammation during *G. parasuis* infection. In future studies, we could validate the expression levels of miR-146a-5p and miR-146a-3p in a larger pig population and perform association analyses with Glässer's disease, aiming to develop miR-146a-5p and miR-146a-3p as biomarkers for the clinical diagnosis of Glässer's disease.

Under baicalin treatment, ssc-miR-27b-5p was the top upregulated miRNA, and ssc-miR-1842 was the top downregulated miRNA with respect to the expression in the *G. parasuis* infection control group. Thus, ssc-miR-27b-5p and ssc-miR-1842 might act as anti-inflammatory factors in the inflammatory response. miR-27b-5p has been reported to protect human umbilical vein endothelial cells against apoptosis [49], inhibit the proliferation and invasion of cutaneous squamous cell carcinoma [50], and restrain the growth and metastatic behaviors of ovarian carcinoma cells [51]. *TLR4* and *Lyn*, target genes of miR-27b-5p, play critical roles in inflammation, tumor pathogenesis, and allergy [52, 53]. However, the effects of miR-1842 have not been described in prior studies. Under probenecid treatment, ssc-miR-1296-5p was the top upregulated miRNA with respect to the expression in the *G. parasuis* infection control group. According to previous studies, miR-1296-5p has tumor-suppressive functions by inhibiting the proliferation, migration, and invasion of human cancer cells [54–56]. Furthermore, the target genes of miR-1296-5p include CDK6, which is a member of nuclear CDKs and is considered to support the expression of proinflammatory mediators [57]. On the basis of prior findings and our results, we inferred

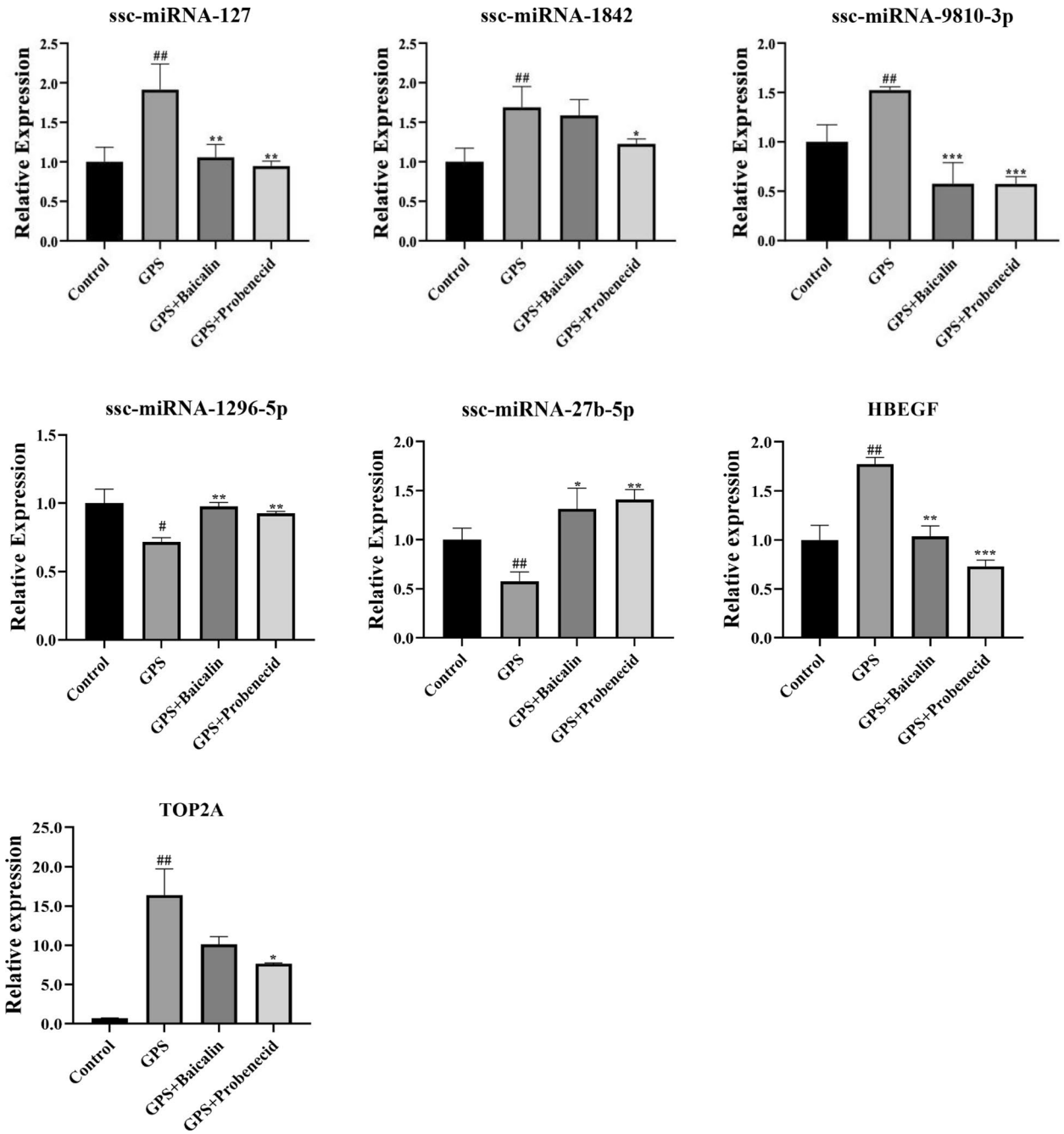

Fig. 7 qRT-PCR validation of differentially expressed genes. GPS: *G. parasuis*-infected PAVECs; GPS + baicalin: *G. parasuis*-infected PAVECs with baicalin pretreatment; GPS + probenecid: *G. parasuis*-infected PAVECs with probenecid treatment. $^{\#}p < 0.05$ and $^{\#\#}p < 0.01$ vs. control; $^{*}p < 0.05$ and $^{**}p < 0.01$ vs. *G. parasuis*-infected PAVECs

that both baicalin and probenecid might alleviate the *G. parasuis*-induced inflammatory response in PAVECs by promoting the expression of key miRNAs, and that miR-27b-5p and miR-1296-5p might serve as new therapeutic targets for *G. parasuis*-induced inflammatory diseases. However, the detailed mechanisms require further study.

When we compared the effects of baicalin and probenecid, ssc-miR-127, ssc-miR-1842, and ssc-miR-9810-3p were the top affected miRNAs in *G. parasuis*-infected PAVECs. The functions of miR-1842 and miR-9810-3p had not been described in previous studies. miR-127 has been reported to suppress cell migration, invasion, and

proliferation in human cancers [58–60]. By targeting various transcription factors and adaptor proteins, miR-127 promotes M1 polarization of macrophages—an important process in immune system regulation—and regulates inflammatory responses [61]. In addition, miR-127 regulates autophagy in the rat hypoxic-ischemic cortex by targeting CISD1, a protein with key roles in regulating cell death and inflammation [62, 63]. Furthermore, another target gene of miR-127, lysine methyltransferase 5A, is involved in the maintenance of a healthy endothelium, through modulating levels of endothelial inflammatory factors in diabetic nephropathy [64, 65]. Consequently, we speculated that miR-127 might be a potential therapeutic target for *G. parasuis*-induced inflammatory responses.

In co-expression analysis, we identified several important functional genes among the targets of DEmiRNAs, including colony-stimulating factor 2 (*CSF2)*, heparin binding EGF like growth factor (*HBEGF)*, exonuclease 1 (*EXO1)*, and DNA topoisomerase II alpha (*TOP2A)* (Fig. 5B). CSF2, a potent cytokine stimulating myeloid cells, induces strong inflammation in retinal degeneration [66], and promotes the transition of macrophages from the M1 to the M2 phenotype in a mouse model of sepsis-induced acute kidney injury [67]. Moreover, HBEGF, produced by group 3 innate lymphoid cells, has been reported to attenuate TNF-mediated epithelial cell death and intestinal inflammation in mice [68]. Interestingly, HBEGF and CSF2 were also found to interact with each other in the PPI network (Fig. 6A), thereby suggesting that HBEGF and CSF2 might be coordinately regulated and participate in modulating the inflammatory response in *G. parasuis*-infected PAVECs. In contrast *EXO1* and *TOP2A* are important genes responsible for DNA replication and superhelix construction. EXO1 resects DNA in the 5′−3′ direction and is involved in many genomic DNA replication processes, such as replication stress response, double strand break repair, mismatch repair, nucleotide excision repair, and telomere maintenance [69]. TOP2A, a topoisomerase modulating the DNA superhelix structure, promotes cell migration, invasion, and epithelial-mesenchymal transition via activating PI3K/AKT signaling in cervical cancer [70]. We observed that EXO1 and TOP2A were two major interacting proteins in the PPI network (Fig. 6). Therefore, perturbation of DNA replication and the DNA superhelix structure might potentially be major causes of the *G. parasuis*-induced inflammation in PAVECs. These findings may provide new directions in research aimed at identifying potent therapeutic targets for Glässer's disease.

In our study, baicalin and probenecid exhibited distinct regulatory patterns on miRNA expression in *G. parasuis*-infected PAVECs. The underlying reason might be attributed to the significant differences in anti-inflammatory mechanisms between baicalin and probenecid. Baicalin could inhibit the release of pro-inflammatory cytokines (such as TNF-α, IL-1β, and IL-6), thereby alleviating inflammatory responses [10]. It is reported that baicalin prevents LPS-induced activation of TLR4/NF-κB p65 pathway and inflammation in mice via inhibiting the expression of CD14 [14]. And our previous work also proved that baicalin could suppress the activation of NF-κB, a crucial transcription factor in inflammatory responses, consequently reducing the expression of inflammation-related genes in pig [16]. However, probenecid is a uric acid excretion promoter primarily used for the treatment of gout, but it also exhibits certain anti-inflammatory properties. One study demonstrated that probenecid effectively mitigates post-ischemic renal injury by synergistically inhibiting the Panx1/P2X7R axis, which inactivates NLRP3 inflammasome signaling and promotes Treg activation in ischemic renal tissues [71]. Thus, baicalin and probenecid may exert anti-inflammatory effects through distinct signaling pathways, which involve different molecules, thereby leading to different impacts on miRNA expression in *G. parasuis*-infected PAVECs in the context of inflammation.

G. parasuis can clinically cause arthritis, meningitis, and polyserositis [1, 2]. However, these conditions are all associated with severe systemic inflammatory responses, with vascular inflammation being the central component of the inflammatory process [1, 2]. Therefore, we aimed to investigate the inflammatory response induced by *G. parasuis* by focusing on the reactions of vascular endothelial cells. In future studies, we could validate the candidate biomarkers in larger pig populations, and expand our research to include multiple cell types and tissue samples to more comprehensively evaluate the systemic impact of *G. parasuis* infection, particularly considering its effects on other organs. Besides, we plan to design experiments with sampling at various time points post-infection, followed by sequencing and functional validation, to investigate the dynamic progression of the infection. Although *G. parasuis* is more clinically prevalent in piglets due to their weaker immune systems, adult pigs are also susceptible to *G. parasuis* infection, and outbreaks in adult populations can result in even greater economic losses. Therefore, future studies should incorporate animal models across different age groups to further explore the influence of age on infection dynamics and treatment effects.

Conclusion

We report the first evidence that both baicalin and probenecid modulate miRNA expression in *G. parasuis*-infected PAVECs. By comparing the effects of

baicalin and probenecid on miRNA expression profiles in PAVECs, we identified microRNA ssc-miR-27b-5p and ssc-miR-1842, hematopoietic cell lineage, insulin resistance, and the AMPK signaling pathways were significantly affected by baicalin, whereas microRNA ssc-miR-9851-3p and ssc-miR-1296-5p, B cell receptor, T cell receptor, and HIF-1 signaling pathways were significantly affected by probenecid. Our findings may serve as a basis for developing new biomarkers and therapeutic targets to control *G. parasuis* infection and may guide future functional research.

Abbreviations

GPS	*Glaesserella parasuis*
miRNAs	MicroRNAs
PAVEC	Porcine aortic vascular endothelial cells
DEmiRNAs	Differentially expressed miRNAs
KEGG	Kyoto Encyclopedia of Genes and Genomes
GO	Gene Ontology
AMPK	AMP-activated protein kinase
PPI	Protein-protein interaction
BA	Baicalin

Supplementary Information

The online version contains supplementary material available at https://doi.org/10.1186/s12917-025-04702-2.

Supplementary Material 1: Supplemental Figure S1. The read length and count distribution in the sequencing data of porcine aortic vascular endothelial cell.

Supplementary Material 2: Supplemental Table S1. Profiles of mature miRNAs identified in twelve libraties.

Supplementary Material 3: Supplemental Table S2. Novel miRNAs identified in the twelve libraries.

Supplementary Material 4: Supplemental Table S3. Differentially expressed miRNAs in G. parasuis-infected PAVECs (group 2 vs. group 1).

Supplementary Material 5: Supplemental Table S4. Differentially expressed miRNAs in G. parasuis-infected PAVECs with baicalin pretreatment (Group 3 vs. Group 2).

Supplementary Material 6: Supplemental Table S5. Differentially expressed miRNAs in G. parasuis-infected PAVECs with probenecid treatment (group 4 vs. group 2).

Supplementary Material 7: Supplemental Table S6. Differentially expressed miRNAs in baicalin treatment group compring to probenecid treatment group (group 3 vs. group 4).

Supplementary Material 8: Supplemental Table S7. Predicted target genes of differentially expressed miRNAs in G. parasuis-infected PAVECs (group 2 vs. group 1).

Supplementary Material 9: Supplemental Table S8. Predicted target genes of differentially expressed miRNAs in G. parasuis-infected PAVECs with baicalin treatment (group 3 vs. group 2).

Supplementary Material 10: Supplemental Table S9. Predicted target genes of differentially expressed miRNAs in G. parasuis-infected PAVECs with probenecid treatment (group 4 vs. group 2).

Supplementary Material 11: Supplemental Table S10. Predicted target genes of differentially expressed miRNAs in baicalin treatment group compring to probenecid treatment group (group 3 vs. group 4).

Supplementary Material 12: Supplemental Table S11. Differential targets of miR-127, miR-1842, and miR-9810-3p.

Authors' contributions
Y.Q. and L.G. conceived and designed the experiments; Y.Y., L.Y., and J.H. performed the experiments; P.S., L.G., S.F., C.Y., and B.Z. analyzed the data; L.G. wrote the paper.

Funding
This work was supported by the National Natural Science Foundation of China (No. 32072917; No. 32273067), and Hubei Key Laboratory of Animal Nutrition and Feed Science, Wuhan Polytechnic University (No. 202301).

Data availability
The datasets generated and/or analyzed during the current study are available in the NCBI Sequence Read Archive (SRA) repository under accession number PRJNA924009.

Declarations

Ethics approval and consent to participate
Animal studies were approved by the Animal Care and Use Committee of Wuhan Polytechnic University, Hubei Province, China (WPU202303002). All experiments were performed in accordance with relevant guidelines and regulations. Written informed consent was obtained from the animal's owner.

Consent for publication
Not applicable.

Competing interests
The authors declare no competing interests.

Author details
[1]School of Animal Science and Nutritional Engineering, Laboratory of Genetic Breeding, Reproduction and Precision Livestock Farming, Wuhan Polytechnic University, Wuhan, Hubei 430023, People's Republic of China. [2]Hubei Key Laboratory of Animal Nutrition and Feed Science, Wuhan Polytechnic University, Wuhan 430023, People's Republic of China. [3]Hubei Collaborative Innovation Center for Animal Nutrition and Feed Safety, Wuhan 430023, People's Republic of China. [4]Hubei Provincial Center of Technology Innovation for Domestic Animal Breeding, Wuhan, Hubei 430023, PR China.

Received: 7 April 2024 Accepted: 20 March 2025
Published: 2 April 2025

References

1. Macedo N, Rovira A, Torremorell M. Haemophilus parasuis: infection, immunity and enrofloxacin. Vet Res. 2015;46:128.
2. Eberle KC, Hau SJ, Luan SL, Weinert LA, Stasko JA, Wang J, et al. Generation and evaluation of a glaesserella (Haemophilus) parasuis capsular mutant. Infect Immun. 2020;88:e00879–919.
3. Ni HB, Gong QL, Zhao Q, Li XY, Zhang XX. Prevalence of Haemophilus parasuis"Glaesserella parasuis" in pigs in China: A systematic review and meta-analysis. Prev Vet Med. 2020;182: 105083.
4. Costa-Hurtado M, Aragon V. Advances in the quest for virulence factors of Haemophilus parasuis. Vet J. 2013;198:571–6.
5. Plantinga NL, Wittekamp BH, van Duijn PJ, Bonten MJ. Fighting antibiotic resistance in the intensive care unit using antibiotics. Fut Microbiol. 2015;10:391–406.
6. Stepanova AY, Solov'eva AI, Malunova MV, Salamaikina SA, Panov YM, Lelishentsev AA. Hairy roots of Scutellaria spp. (Lamiaceae) as promising producers of antiviral flavones. Molecules. 2021;26:3927.
7. Luo J, Dong B, Wang K, Cai S, Liu T, Cheng X, et al. Baicalin inhibits biofilm formation, attenuates the quorum sensing-controlled virulence and enhances Pseudomonas aeruginosa clearance in a mouse peritoneal implant infection model. PLoS ONE. 2017;12: e0176883.
8. Xu M, Li X, Song L. Baicalin regulates macrophages polarization and alleviates myocardial ischaemia/reperfusion injury via inhibiting JAK/STAT pathway. Pharm Biol. 2020;58:655–63.

9. Yang J, Yang X, Yang J, Li M. Baicalin ameliorates lupus autoimmunity by inhibiting differentiation of Tfh cells and inducing expansion of Tfr cells. Cell Death Dis. 2019;10:140.
10. Guo L, Liu J, Zhang Y, Fu S, Qiu Y, Ye C, et al. The effect of baicalin on the expression profiles of long non-coding RNAs and mRNAs in Porcine aortic vascular endothelial cells infected with Haemophilus parasuis. DNA Cell Biol. 2020;39:801–15.
11. Lei K, Shen Y, He Y, Zhang L, Zhang J, Tong W, et al. Baicalin Represses C/EBPbeta via Its Antioxidative Effect in Parkinson's Disease. Oxid Med Cell Longev. 2020;2020:8951907.
12. Wang X, Chang X, Zhan H, Zhang Q, Li C, Gao Q, et al. Curcumin and Baicalin ameliorate ethanol-induced liver oxidative damage via the Nrf2/HO-1 pathway. J Food Biochem. 2020;44(10):e13425.
13. Zhou W, Gao M, Liang C, Lin B, Wu Q, Chen R, et al. Systematic understanding of the mechanism of baicalin against gastric cancer using transcriptome analysis. Biomed Res Int. 2021;2021:5521058.
14. Fu YJ, Xu B, Huang SW, Luo X, Deng XL, Luo S, et al. Baicalin prevents LPS-induced activation of TLR4/NF-kappaB p65 pathway and inflammation in mice via inhibiting the expression of CD14. Acta Pharmacol Sin. 2021;42:88–96.
15. Yan G, Chen L, Wang H, Wu S, Li S, Wang X. Baicalin inhibits LPS-induced inflammation in RAW264.7 cells through miR-181b/HMGB1/TRL4/NF-kappaB pathway. Am J Transl Res. 2021;13:10127–41.
16. Fu S, Liu H, Xu L, Qiu Y, Liu Y, Wu Z, et al. Baicalin modulates NF-kappaB and NLRP3 inflammasome signaling in porcine aortic vascular endothelial cells Infected by Haemophilus parasuis Causing Glasser's disease. Sci Rep. 2018;8:807.
17. Fu S, Liu J, Xu J, Zuo S, Zhang Y, Guo L, et al. The effect of baicalin on microRNA expression profiles in porcine aortic vascular endothelial cells infected by Haemophilus parasuis. Mol Cell Biochem. 2020;472:45–56.
18. Cunningham RF, Israili ZH, Dayton PG. Clinical pharmacokinetics of probenecid. Clin Pharmacokinet. 1981;6:135–51.
19. Robbins N, Koch SE, Tranter M, Rubinstein J. The history and future of probenecid. Cardiovasc Toxicol. 2012;12:1–9.
20. Rawson TM, Wilson RC, O'Hare D, Herrero P, Kambugu A, Lamorde M, et al. Optimizing antimicrobial use: challenges, advances and opportunities. Nat Rev Microbiol. 2021;19:747–58.
21. Ibrahim E, Aballa TC, Lynne CM, Brackett NL. Oral probenecid improves sperm motility in men with spinal cord injury. J Spinal Cord Med. 2018;41:567–70.
22. Colin-Gonzalez AL, Santamaria A. Probenecid: an emerging tool for neuroprotection. CNS Neurol Disord Drug Targets. 2013;12:1050–65.
23. Vamos E, Voros K, Zadori D, Vecsei L, Klivenyi P. Neuroprotective effects of probenecid in a transgenic animal model of Huntington's disease. J Neural Transm (Vienna). 2009;116:1079–86.
24. Williams G, Gatt A, Clarke E, Corcoran J, Doherty P, Chambers D, et al. Drug repurposing for Alzheimer's disease based on transcriptional profiling of human iPSC-derived cortical neurons. Transl Psychiatry. 2019;9:220.
25. Tripp RA, Martin DE. Repurposing Probenecid to Inhibit SARS-CoV-2, Influenza Virus, and Respiratory Syncytial Virus (RSV) Replication. Viruses. 2022;14: 612.
26. Murray J, Bergeron HC, Jones LP, Reener ZB, Martin DE, Sancilio FD, et al. Probenecid Inhibits Respiratory Syncytial Virus (RSV) Replication. Viruses. 2022;14: 912.
27. Wonnenberg B, Tschernig T, Voss M, Bischoff M, Meier C, Schirmer SH, et al. Probenecid reduces infection and inflammation in acute Pseudomonas aeruginosa pneumonia. Int J Med Microbiol. 2014;304:725–9.
28. Zhanel GG, Pozdirca M, Golden AR, Lawrence CK, Zelenitsky S, Berry L, et al. Sulopenem: an intravenous and oral penem for the treatment of urinary tract infections due to multidrug-resistant bacteria. Drugs. 2022;82:533–57.
29. Lu TX, Rothenberg ME. MicroRNA. J Allergy Clin Immunol. 2018;141:1202–7.
30. Mohr AM, Mott JL. Overview of microRNA biology. Semin Liver Dis. 2015;35:3–11.
31. Lin HY, Yang YL, Wang PW, Wang FS, Huang YH. The Emerging Role of MicroRNAs in NAFLD: highlight of MicroRNA-29a in modulating oxidative stress, inflammation, and beyond. Cells. 2020;9: 1041.
32. Singh RP, Massachi I, Manickavel S, Singh S, Rao NP, Hasan S, et al. The role of miRNA in inflammation and autoimmunity. Autoimmun Rev. 2013;12:1160–5.
33. Tili E, Michaille JJ, Piurowski V, Rigot B, Croce CM. MicroRNAs in intestinal barrier function, inflammatory bowel disease and related cancers-their effects and therapeutic potentials. Curr Opin Pharmacol. 2017;37:142–50.
34. Wang C, Zhang C, Liu L, Xi A, Chen B, Li Y, et al. Macrophage-derived mir-155-containing exosomes suppress fibroblast proliferation and promote fibroblast inflammation during cardiac injury. Mol Ther. 2017;25:192–204.
35. Neudecker V, Yuan X, Bowser JL, Eltzschig HK. MicroRNAs in mucosal inflammation. J Mol Med (Berl). 2017;95:935–49.
36. Guo L, Tsai SQ, Hardison NE, James AH, Motsinger-Reif AA, Thames B, et al. Differentially expressed microRNAs and affected biological pathways revealed by modulated modularity clustering (MMC) analysis of human preeclamptic and IUGR placentas. Placenta. 2013;34:599–605.
37. Su Y, Yuan J, Zhang F, Lei Q, Zhang T, Li K, et al. MicroRNA-181a-5p and microRNA-181a-3p cooperatively restrict vascular inflammation and atherosclerosis. Cell Death Dis. 2019;10:365.
38. Cai Y, Zhang Y, Chen H, Sun XH, Zhang P, Zhang L, et al. MicroRNA-17-3p suppresses NF-kappaB-mediated endothelial inflammation by targeting NIK and IKKbeta binding protein. Acta Pharmacol Sin. 2021;42:2046–57.
39. Guo L, Xu L, Wu T, Fu S, Qiu Y, Hu CA, et al. Evaluation of recombinant protein superoxide dismutase of Haemophilus parasuis strain SH0165 as vaccine candidate in a mouse model. Can J Microbiol. 2017;63:312–20.
40. Kim S, Kang D, Huo Z, Park Y, Tseng GC. Meta-analytic principal component analysis in integrative omics application. Bioinformatics. 2018;34:1321–8.
41. Robinson MD, McCarthy DJ, Smyth GK. edgeR: a Bioconductor package for differential expression analysis of digital gene expression data. Bioinformatics. 2010;26:139–40.
42. Gene OC. Gene ontology consortium: going forward. Nucleic Acids Res. 2015;43:D1049–56.
43. Kanehisa M, Goto S. KEGG: kyoto encyclopedia of genes and genomes. Nucleic Acids Res. 2000;28:27–30.
44. Huang Y, Ma XY, Yang YB, Ren HT, Sun XH, Wang LR. Identification and characterization of microRNAs and their target genes from Nile tilapia (Oreochromis niloticus). Z Naturforsch C J Biosci. 2016;71:215–23.
45. Choi YJ, Kim C, Choi EW, Lee SH, Chae MK, Jun HO, et al. MicroRNA-155 acts as an anti-inflammatory factor in orbital fibroblasts from Graves' orbitopathy by repressing interleukin-2-inducible T-cell kinase. PLoS ONE. 2022;17: e0270416.
46. Chen X, Li W, Chen T, Ren X, Zhu J, Hu F, et al. miR-146a-5p promotes epithelium regeneration against LPS-induced inflammatory injury via targeting TAB1/TAK1/NF-kappaB signaling pathway. Int J Biol Macromol. 2022;221:1031–40.
47. Hua T, Yang M, Song H, Kong E, Deng M, Li Y, et al. Huc-MSCs-derived exosomes attenuate inflammatory pain by regulating microglia pyroptosis and autophagy via the miR-146a-5p/TRAF6 axis. J Nanobiotechnology. 2022;20:324.
48. Yang Y, Li L. Depleting microRNA-146a-3p attenuates lipopolysaccharide-induced acute lung injury via up-regulating SIRT1 and mediating NF-kappaB pathway. J Drug Target. 2021;29:420–9.
49. Pan YK, Li CF, Gao Y, Wang YC, Sun XQ. Effect of miR-27b-5p on apoptosis of human vascular endothelial cells induced by simulated microgravity. Apoptosis. 2020;25:73–91.
50. Liang D, Zhang Z. MicroRNA-27b-3p inhibits the proliferation and invasion of cutaneous squamous cell carcinoma by targeting EGFR and MMP-13. Oncol Lett. 2021;22:729.
51. Liu CH, Jing XN, Liu XL, Qin SY, Liu MW, Hou CH. Tumor-suppressor miRNA-27b-5p regulates the growth and metastatic behaviors of ovarian carcinoma cells by targeting CXCL1. J Ovarian Res. 2020;13:92.
52. Zhang P, Yang M, Chen C, Liu L, Wei X, Zeng S. Toll-Like Receptor 4 (TLR4)/Opioid Receptor Pathway Crosstalk and Impact on Opioid Analgesia, Immune Function, and Gastrointestinal Motility. Front Immunol. 2020;11: 1455.
53. Sun Y, Yang Y, Zhao Y, Li X, Zhang Y, Liu Z. The role of the tyrosine kinase Lyn in allergy and cancer. Mol Immunol. 2021;131:121–6.
54. Shan X, Wen W, Zhu D, Yan T, Cheng W, Huang Z, et al. miR 1296–5p Inhibits the Migration and Invasion of Gastric Cancer Cells by Repressing ERBB2 Expression. PLoS ONE. 2017;12: e0170298.
55. Jia Y, Zhao LM, Bai HY, Zhang C, Dai SL, Lv HL, et al. The tumor-suppressive function of miR-1296-5p by targeting EGFR and CDK6 in gastric cancer. Biosci Rep. 2019;39:BSR20181556.

56. Wang L, Hu K, Chao Y, Wang X. MicroRNA-1296-5p suppresses the proliferation, migration, and invasion of human osteosarcoma cells by targeting NOTCH2. J Cell Biochem. 2020;121:2038–46.
57. Schmitz ML, Kracht M. Cyclin-dependent kinases as coregulators of inflammatory gene expression. Trends Pharmacol Sci. 2016;37(2):101–13.
58. Wang L, Wang X, Jiang X. miR-127 suppresses gastric cancer cell migration and invasion via targeting Wnt7a. Oncol Lett. 2019;17:3219–26.
59. Du SY, Huang XX, Li NM, Lv CY, Lv CH, Wei ML, et al. MiR-127-3p inhibits proliferation of ovarian cancer in rats through down-regulating MAPK4. Eur Rev Med Pharmacol Sci. 2020;24:10383–90.
60. Liu X, Meng Z, Xing Y, Zhong Q, Zhang X, Qu J. MiR-127 inhibits ovarian cancer migration and invasion by up-regulating ITGA6. Minerva Med. 2021;112:309–10.
61. Essandoh K, Li Y, Huo J, Fan GC. MiRNA-Mediated Macrophage Polarization and its Potential Role in the Regulation of Inflammatory Response. Shock. 2016;46:122–31.
62. Zhang ZB, Xiong LL, Xue LL, Deng YP, Du RL, Hu Q, et al. MiR-127-3p targeting CISD1 regulates autophagy in hypoxic-ischemic cortex. Cell Death Dis. 2021;12:279.
63. Hua J, Gao Z, Zhong S, Wei B, Zhu J, Ying R. CISD1 protects against atherosclerosis by suppressing lipid accumulation and inflammation via mediating Drp1. Biochem Biophys Res Commun. 2021;577:80–8.
64. Huang T, Li X, Wang F, Lu L, Hou W, Zhu M, et al. The CREB/KMT5A complex regulates PTP1B to modulate high glucose-induced endothelial inflammatory factor levels in diabetic nephropathy. Cell Death Dis. 2021;12:333.
65. Yuan R, Zhang X, Fang Y, Nie Y, Cai S, Chen Y, et al. mir-127-3p inhibits the proliferation of myocytes by targeting KMT5a. Biochem Biophys Res Commun. 2018;503:970–6.
66. Saita K, Moriuchi Y, Iwagawa T, Aihara M, Takai Y, Uchida K, et al. Roles of CSF2 as a modulator of inflammation during retinal degeneration. Cytokine. 2022;158: 155996.
67. Li Y, Zhai P, Zheng Y, Zhang J, Kellum JA, Peng Z. Csf2 Attenuated Sepsis-Induced Acute Kidney Injury by Promoting Alternative Macrophage Transition. Front Immunol. 2020;11: 1415.
68. Zhou L, Zhou W, Joseph AM, Chu C, Putzel GG, Fang B, et al. Group 3 innate lymphoid cells produce the growth factor HB-EGF to protect the intestine from TNF-mediated inflammation. Nat Immunol. 2022;23:251–61.
69. Sertic S, Quadri R, Lazzaro F, Muzi-Falconi M. EXO1: A tightly regulated nuclease. DNA Repair (Amst). 2020;93: 102929.
70. Wang B, Shen Y, Zou Y, Qi Z, Huang G, Xia S, et al. TOP2A promotes cell migration, invasion and epithelial-mesenchymal transition in cervical cancer via activating the PI3K/AKT signaling. Cancer Manag Res. 2020;12:3807–14.
71. El-Maadawy WH, Hassan M, Badawy MH, AbuSeada A, Hafiz E. Probenecid induces the recovery of renal ischemia/reperfusion injury via the blockade of Pannexin 1/P2X7 receptor axis. Life Sci. 2022;308: 120933.

Publisher's Note